2-1-2020

Galaxy and Mass Assembly (GAMA): Defining passive galaxy samples and searching for the UV upturn

S. Phillipps
University of Bristol

S. S. Ali
University of Bristol

M. N. Bremer
University of Bristol

R. de Propris
Turun yliopisto

A. E. Sansom
University of Central Lancashire

See next page for additional authors

Authors

S. Phillipps, S. S. Ali, M. N. Bremer, R. de Propris, A. E. Sansom, M. E. Cluver, M. Alpaslan, S. Brough, M. J.I. Brown, L. J.M. Davies, S. P. Driver, M. W. Grootes, Benne W. Holwerda, A. M. Hopkins, P. A. James, K. Pimbblet, A. S.G. Robotham, E. N. Taylor, and L. Wang

Galaxy And Mass Assembly (GAMA): Defining Passive Galaxy Samples and Searching for the UV Upturn

S. Phillipps[1], S.S. Ali[1,2], M.N. Bremer[1], R. De Propris[3], A.E. Sansom[4], M.E. Cluver[5,6],
M. Alpaslan[7], S. Brough[8], M.J.I. Brown[9], L.J.M. Davies[10], S.P. Driver[10,11], M.W. Grootes[12],
B.W. Holwerda[13], A.M. Hopkins[14], P.A. James[15], K. Pimbblet[16], A.S.G. Robotham[10],
E.N. Taylor[5] and L. Wang[17,18]

[1]*Astrophysics Group, School of Physics, University of Bristol, Tyndall Avenue, Bristol, BS8 1TL, UK*
[2]*Subaru Telescope, NAOJ, 650 North A'ohoku Place, Hilo, HI 96720, USA*
[3] *Finnish Centre for Astronomy with ESO, University of Turku, Vesilinnantie 5, 21400, Turku, Finland*
[4]*Jeremiah Horrocks Institute, School of Physical Sciences and Computing, University of Central Lancashire, Preston PR1 2HE, UK*
[5]*Centre for Astrophysics and Supercomputing, Swinburne University of Technology, Hawthorn, VIC 3122, Australia*
[6]*Department of Physics and Astronomy, University of the Western Cape, Robert Sobukwe Road, Belville 7535, South Africa*
[7]*Center for Cosmology and Particle Physics, Department of Physics, New York University, NY 10012, USA*
[8]*School of Physics, University of New South Wales, NSW 2052, Australia*
[9]*School of Physics and Astronomy, Monash University, Clayton, Victoria 3800, Australia*
[10]*ICRAR, University of Western Australia, 35 Stirling Highway, Crawley, WA 6009, Australia*
[11]*SUPA, School of Physics and Astronomy, University of St Andrews, North Haugh, St Andrews, Fife KY16 9SS, UK*
[12]*Netherlands eScience Center, Science Park 140, 1098 XG Amsterdam, The Netherlands*
[13]*Department of Physics and Astronomy, 102 Natural Science Building, University of Louisville, Louisville KY 40292, USA*
[14]*Australian Astronomical Optics, Macquarie University, 105 Delhi Road, North Ryde, NSW 2113, Australia*
[15]*Astrophysics Research Institute, Liverpool John Moores University, IC2, Liverpool Science Park, 146 Brownlow Hill, Liverpool L3 5RF, UK*
[16]*E.A. Milne Centre for Astrophysics, University of Hull, Cottingham Road, Kingston-upon-Hull HU6 7RX, UK*
[17]*SRON Netherlands Institute for Space Research, Landleven 12, 9747 AD Groningen, The Netherlands*
[18]*Kapteyn Astronomical Institute, University of Groningen, Postbus 800, 9700 AV Groningen, The Netherlands*

ABSTRACT

We use data from the GAMA and GALEX surveys to demonstrate that the UV upturn, an unexpected excess of ultraviolet flux from a hot stellar component, seen in the spectra of many early-type galaxies, arises from processes internal to individual galaxies with no measurable influence from the galaxies' larger environment. We first define a clean sample of passive galaxies without a significant contribution to their UV flux from low-level star formation. We confirm that galaxies with the optical colours of red sequence galaxies often have signs of residual star formation, which, without other information, would prevent a convincing demonstration of the presence of UV upturns. However, by including (NUV$-u$) and *WISE* (W2-W3) colours, and FUV data where it exists, we can convincingly constrain samples to be composed of non-star-forming objects. Using such a sample, we examine GALEX photometry of low redshift GAMA galaxies in a range of low-density environments, from groups to the general field, searching for UV upturns. We find a wide range of (NUV$-r$) colours, entirely consistent with the range seen – and attributed to the UV upturn – in low-redshift red sequence cluster galaxies. The range of colours is independent of group multiplicity or velocity dispersion, with isolated passive galaxies just as likely to have blue UV-to-optical colours, implying significant upturn components, as those in richer groups and in the previous data on clusters. This is supported by equivalent results for (FUV$-r$) colours which are clear indicators of upturn components.

Key words: galaxies: evolution – galaxies: stellar content – galaxies: star formation

1 INTRODUCTION

The 'UV upturn' signifies the *a priori* unexpected excess of ultraviolet flux seen in the spectra of many early-type galaxies, compared

to what would be expected for a conventional old, metal-rich stellar population (Code & Welch 1979; Bertola et al. 1982; O'Connell 1999). The upturn is therefore commonly attributed to a minority old but hot stellar population, such as hot horizontal branch stars (Greggio & Renzini 1990; Yi et al. 1998), with a helium-enhanced population often being posited (e.g. Norris 2004; Lee et al. 2005; Chung et al. 2011). Although Burstein et al. (1988) early on reported an upturn in several nearby fairly isolated ellipticals such as NGC 4697, almost all subsequent work concentrated on early-type galaxies in rich clusters such as Virgo (Boselli et al. 2005) or Coma (Smith et al. 2012), and generally on only the brighter cluster members (e.g. Brown et al. 2000, 2003).

More recently Ali et al. (2018a,b,c) have demonstrated that the upturn is common in early-type galaxies in clusters across a broad range of galaxy luminosities, in a wide variety of clusters with different physical properties, at different redshifts (see also Ali et al. 2019). This appears to indicate that the phenomenon is internal to the stellar populations of many individual passive galaxies, with a range of (reasonably old) ages, with no obvious environmental effects at play. In their work, they created reasonably well-sampled ultraviolet spectral energy distributions (SEDs) from a combination of photometry from different sources (GALEX, UVOT and SDSS). The spectral shapes which they determined then enabled them to rule out (significant) contributions to the UV flux from star formation in their sample of objects and hence demonstrate the presence of upturn components. However, for most large-scale galaxy surveys, this level of detail in the UV SED will not generally be available. We will therefore need to eliminate star-forming galaxies from samples of potential (passive) upturn galaxies by other means, such as using multiple broad-band colours.

In the present paper we use low redshift ($z < 0.05$) galaxies from the Galaxy And Mass Assembly (GAMA) survey (Driver et al. 2011; Liske et al. 2015; Baldry et al. 2018) to explore the best means of extracting purely passive galaxy samples via the wide range of available broad-band photometry. We then use such a sample to investigate whether UV upturns exist in the spectra of early type galaxies in groups and the field and, if so, whether they have the same range of strengths, as represented by near- and far-UV to optical colours, as early types in clusters. NUV and FUV data for our sample galaxies are obtained from the GALEX catalogues, which have been previously cross-matched to the GAMA catalogues as described in Liske et al. (2015).

We further take advantage of the rich panchromatic survey data in GAMA (Driver et al. 2016) to explore the characteristics of (optical) red sequence galaxies in general, and those which are candidates for totally passive early-types with UV upturns in particular. Besides the observed and rest-frame magnitudes across a wide range of bands, including particularly the mid-infrared from *WISE* (Cluver et al. 2014) and far-infrared from *Herschel* (Eales et al. 2015), the GAMA database provides fits to the multi-wavelength SEDs made using stellar population synthesis techniques (Taylor et al. 2011; Driver et al. 2016; Wright et al. 2016).

All magnitudes used in this work are in the AB system. Where relevant we use $H_0 = 70$ kms^{-1}Mpc^{-1}, $\Omega_{\rm m} = 0.3$ and $\Omega_\Lambda = 0.7$ as in Taylor et al. (2011) from whose (updated) catalogue we take our basic GAMA parameters.

2   SAMPLE SELECTION

The GAMA survey is based on a highly complete galaxy redshift survey (Baldry et al. 2010; Hopkins et al. 2013; Liske et al. 2015; Baldry et al. 2018) covering approximately 280 deg^2 to a main survey magnitude limit of $r < 19.8$. This area is split into three equatorial (G09, G12 and G15) and two southern (G02 and G23) regions. In the present work we use galaxies from the three equatorial fields. The spectroscopic survey was undertaken with the AAOmega fibre-fed spectrograph (Saunders et al. 2004; Sharp et al. 2006) allied to the Two-degree Field (2dF) fibre positioner on the Anglo-Australian Telescope (Lewis et al. 2002). It obtained redshifts for $\sim 300,000$ targets covering $0 < z < 0.6$, with a median redshift of $z \simeq 0.2$, with high (and uniform) spatial completeness (98.5%) on the sky in the GAMA equatorial areas (Robotham et al. 2010). A total of 195,669 galaxies have high quality spectra (GAMA redshift quality code nQ> 2) in the GAMA catalogues

Built around the redshift survey, photometric data are provided at a wide range of wavelengths from the far-ultraviolet to far-infrared. Full details can be found in Driver et al. (2011, 2016) and Liske et al. (2015).

Within the multi-wavelength database, each galaxy is also characterised by a wide range of derived parameters. Those of interest in the current work include rest-frame magnitudes and colours, stellar masses and other stellar population parameters, derived from multi-wavelength SED fitting (Taylor et al. 2011). The fits themselves are made across the *rest-frame* wavelength range 3000-10000 Å. They assume Bruzual & Charlot (2003) models with a Chabrier (2003) stellar initial mass function and with a variety of possible metallicities, and include allowance for the effects of dust extinction via a Calzetti et al. (2000) extinction curve. Further interstellar medium (ISM) and star formation properties are derived via a MAGPHYS (da Cunha, Charlot & Elbaz 2008) analysis of a wide range of photometric measures from the far-UV to far-IR (Driver et al. 2016; Wright et al. 2016).

For comparison with low redshift cluster data (Ali et al. 2018a, 2019), we select galaxies with (flow-corrected: Tonry et al. 2000; Baldry et al. 2012) redshifts $0.002 < z < 0.05$. As we wish to study moderate-to-high luminosity objects (again for comparison with the local cluster samples) we choose to limit luminosities to $M_r < -19$. Note that this also ensures that we have a securely volume complete sample; GAMA is spectroscopically complete to below $M_r = -17.5$ at our maximum distance. Furthermore, the combination of low redshift and high luminosity provides the best prospect of the required ultraviolet and mid-infrared photometry having small errors. At these redshifts k-corrections in the UV are small enough to be neglected relative to the photometric errors (less than about 0.1 mags, see Ali et al. 2019; Kaviraj et al. 2007a), while k-corrections in the optical are already taken into account in the data. Look-back times are all less than 0.7 Gyr, so evolutionary effects across the sample depth will be very small: at moderate to old ages the Conroy, Gunn & White (2009) models used by Ali et al. (2018a), for instance, evolve by only 0.03 magnitudes in $(U-V)$ per Gyr (see also Phillipps et al. 2019).

To explore the UV upturn we require at least a 5-sigma detection of a given galaxy (equivalent to a magnitude error less than 0.2) in the GALEX NUV band at central wavelength 232 nm; the FUV band observations at 154 nm are less deep (Morrissey et al. 2007). The matching of GAMA and GALEX detections is discussed in detail in Section 4.2 of Liske et al. (2015), who demonstrate that the GALEX detection rate (for typical exposure times of 1500 s) is better than 80% for low-redshift galaxies of all types brighter than $r = 18$, which covers all our galaxies. With the 5-sigma limit, this leaves us with 797 GALEX objects.

As we are interested in the environments of our galaxies (Brough et al. 2013), we also match them to the GAMA group
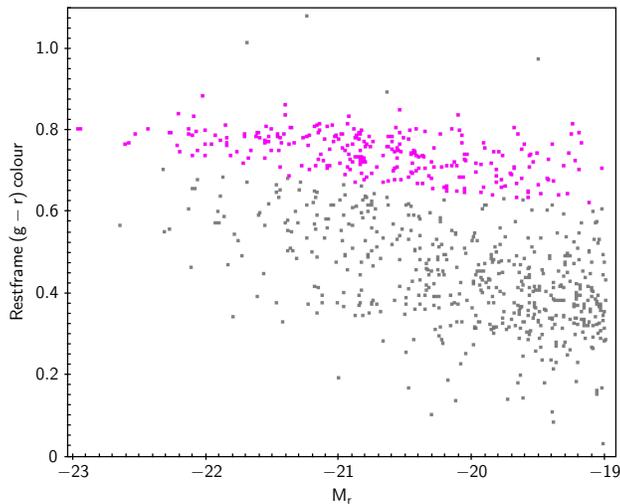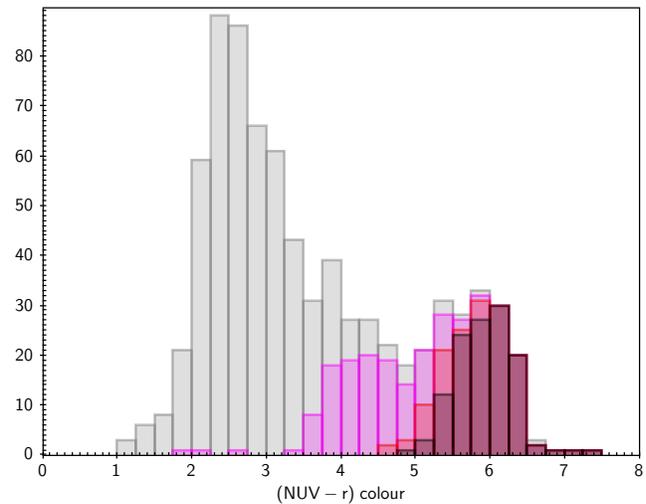
Figure 1. Standard optical rest-frame $(g - r)$ versus M_r colour magnitude diagram for our overall sample of 773 nearby bright galaxies. The objects picked out in pink comprise the initial optical red sequence selection of 265 galaxies, grey points are the remainder, i.e. essentially blue cloud objects. Photometric errors in $(g-r)$ are less than 0.05 magnitudes and those in M_r are around 0.02 magnitudes.

Figure 2. Distribution of rest-frame $(NUV-r)$ colours for our overall sample of nearby bright galaxies (grey) and the initial optical red sequence selected sample of galaxies (pink). The colour errors are around 0.2 magnitudes. The red histogram shows the distribution for the red sequence galaxies after the use of the additional cut in $(NUV -u)$ as discussed in Section 3.1 (the NUV red sequence sample with 147 objects) and the dark red (black bordered) histogram shows the 122 objects remaining after a further cut on *WISE* (W2−W3) colour (the NUV+*WISE* red sequence sample from Section 3.2).

catalogue (G3C: Robotham et al. 2011). This further requirement leaves us with a sample of 773 nearby bright NUV-detected galaxies (after one object with an implausible $(g-r)$ colour is removed). Structural parameters from Sérsic profile fits (Kelvin et al. 2012) and morphological type classifications (Kelvin et al. 2014; Moffett et al. 2016) are also utilised.

3 THE RED SEQUENCE

The standard procedure for selecting passive galaxies is to use the split between the 'red sequence' and 'blue cloud' (e.g. Baldry et al. 2004 *et seq.*) in an optical colour-magnitude diagram, e.g. $(g - r)$ versus M_r. We display this for our sample galaxies in Fig. 1. Note that g and r have been corrected to the rest frame but have not been corrected for any internal dust reddening. The slope of our red sequence ($\simeq -0.03$) is consistent with numerous other local determinations and the width of the region chosen is ± 0.1 magnitudes, following De Propris (2017) and De Propris et al. (2018). This optical red sequence sample contains 265 galaxies.

The UV upturn in passive galaxies is conventionally quantified by a UV-to-optical colour, usually $(NUV-r)$ or $(FUV-r)$ as in, e.g., Smith et al. (2012) and Ali et al. (2019). Although using the FUV is preferable in some ways (having a longer lever arm into the upturn region, e.g. Dorman, O'Connell & Rood 2003), coverage is sparser and $(NUV-r)$ is still a good proxy for the upturn strength. The upturn component contributes significant light, alongside the normal old stars, at least to 2800Å (Burstein et al. 1988; Dorman, O'Connell & Rood 1995; Smith et al. 2012) (recall that our NUV band is around 2300Å). Burstein et al. (1988) originally discussed the steeply rising flux below 2000Å in some early type galaxies, but also noted that this hot component affected the whole spectrum shortward of 3200Å. In general terms, the minimum in the SED around 2500Å in typical passive galaxy spectra does not indicate that the hot component is unimportant at these wavelengths, but that this is the cross-over point between the steeply declining old component and the steeply rising hot component, i.e. where the

two components are roughly equally important (see e.g. Yi et al. 1998; Dorman, O'Connell & Rood 2003, figure 1). A detailed consideration of the spectral components, as in Ali et al. (2018a), using models of old, high metallicity populations from Conroy, Gunn & White (2009), implies that there is relatively little flux from the old component below 2800Å (see also Dorman, O'Connell & Rood 2003). Dorman, O'Connell & Rood (1995, 2003) noted that for strong UV sources (with no star formation) the contribution of the hot (horizontal branch) population to the 2500Å flux is around 75-80%.

Fig. 2 shows the distribution of $(NUV-r)$ colour for our total sample (in grey) and for the optical red sequence galaxies (pink). It is immediately apparent that, as is well known, the optical red sequence is significantly contaminated by galaxies with the NUV-optical colours of star-forming galaxies, i.e. $(NUV-r)$ less than about 5 (see e.g. Kaviraj et al. 2007a; Kaviraj 2010; Crossett et al. 2017). These are interpreted as early-type galaxies with residual star formation (e.g. Salim & Rich 2010) or 'red spirals' with strongly suppressed star formation (e.g. Crossett et al. 2014).[1]

This already indicates that, following Yi et al. (2005), Salim & Rich (2010) and Salim (2014) for instance, we can obtain a cleaner passive sequence by cutting at around $(NUV-r) = 5$, where we see a clear minimum in the distribution of UV-optical colours. Crossett et al. (2014) use a stricter cut at $(NUV-r) = 5.4$ to separate out galaxies in rich clusters with residual star formation.

In the specific context of upturn galaxies, Yi et al. (2011) required a combination of $(NUV -r) > 5.4$, $(FUV-NUV) < 0.9$ and $(FUV -r) < 6.6$ in order for a galaxy to count as non-star forming with an upturn. However, this – and specifically the very

---

[1] Optical red sequence galaxies may also include interlopers with significant star formation but strong dust reddening (e.g. Sodré et al. 2013), which will be red in all colours.

blue (FUV-NUV) limit – appears to be based on a particular assumption for the temperature of the stars contributing to the UV upturn and returned no candidates in the Coma cluster, clearly in disagreement with other work. Based on the spectra of apparently passive galaxies, Smith et al. (2012) suggest that a 'continuous' consideration of the colours is to be preferred, rather than Yi et al.'s imposition of discrete limits (see also Ali et al. 2018a), with the (FUV-NUV) colours of their passive objects ranging up to about 2 (see also Brown et al. 2014). Rich et al. (2005) had previously also found a wide range of (FUV-NUV) for (spectroscopically) quiescent early type galaxies (see also Donas et al. 2007; Carter et al. 2011). On the other hand, Rich et al.'s wide range of (FUV$-r$) colours for quiescent galaxies strongly overlapped with those of star forming galaxies at (FUV$-r$) < 6 (their Figure 1), suggesting that residual effects of low-level star formation can be present even when no measurable emission lines are evident.

Arnouts et al. (2013) compared specific star formation rates (sSFRs) for their $z < 0.2$ GALEX and SWIRE detected galaxies, as derived from UV to mid-IR SED fitting, to their positions in a (NUV$-r$) versus ($r - K$) colour-colour diagram. They found that galaxies with red (NUV$-r$) for their ($r - K$) had a low mean sSFR, with a clear subset of their galaxies falling in this quadrant, well separated from the blue star forming galaxies. However, while centred on (NUV$-r$) $\simeq 5$ their selection included objects as blue as (NUV$-r$) $\simeq 4$ and only removed objects with sSFR $< 10^{-10.5}$yr^{-1}, which is insufficiently tight if we wish to isolate the effects of a genuine UV upturn. Rawle et al. (2008) had similarly used NUV and the infrared J band, again finding a wide colour spread, though not associating it with an upturn component. (See also Leja et al. 2019, for a recent extension of the UBJ method, though for high z galaxies).

In any case, the existence of two roughly Gaussian distributions in the bimodal overall (NUV$-r$) colour distribution cautions (cf. Taylor et al. 2015) that some objects with residual star formation may still exist at (NUV$-r$) > 5. With these considerations in mind, in order to investigate further the selection of truly passive galaxies (with or without UV upturns), we next consider additional constraints from a broad range of other colours.

3.1 The UV Spectral Slope

First we could consider simply using a selection on ($u - r$), which is known to correlate reasonably well with sSFR (e.g. Bremer et al. 2018). However, in practice this makes virtually no difference, the ($g-r$) selected objects remain on the ($u-r$) red sequence (cf. the tight correlation of ($u - g$) with ($g - r$) for early-type galaxies in Figure 5 of Brown et al. 2014, for instance). We therefore need to consider shorter wavelengths than u, where the sensitivity to star formation is greater (e.g. Schawinski et al. 2007).

In general terms, the SED of non-star-forming 'upturn galaxies' will have red optical colours and an inflection below the $u-$band, before rising again (or, strictly, changing the SED slope upwards) at shorter wavelengths. By comparison, completely passive galaxies with no upturn population will have strongly declining flux from the u to the NUV. Finally, any star-forming component will have, or add, a roughly flat spectrum at short wavelengths, while the galaxy's optical colours will be generated by the combination of young and old populations (cf. the various model spectra in Hernández-Pérez & Bruzual 2014, for instance). Together, this implies that, for upturn galaxies, we should be looking for galaxies which are bluer in (NUV$-r$) or (NUV$-u$) than the standard pas-
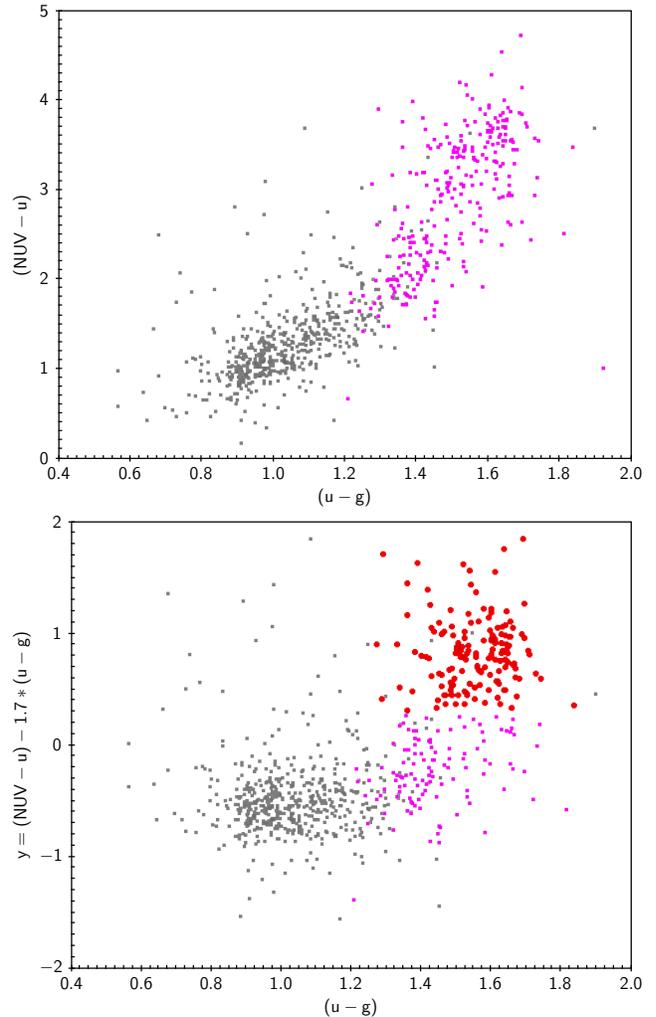
Figure 3. Top panel: The distribution of rest-frame (NUV$-u$) versus ($u - g$) colours for our overall sample (grey). The objects picked out in pink comprise the initial optical red sequence selection. Bottom panel: Same but using the 'rectified' colour y, defined as the (NUV$-u$) colour relative to its trend with ($u - g$) for star-forming galaxies (so that star-forming galaxies have the same mean y at all ($u-g$), see text). Galaxies marked by red circles show our more stringent NUV red sequence selection. Photometric errors are around 0.07 magnitudes in ($u - g$) and 0.2 magnitudes in (NUV$-u$).

sive models, yet not so blue as galaxies with (even small amounts of) star formation.

In Fig. 3 we therefore plot, in the top panel, the diagnostic colour-colour diagram (NUV $-u$) versus ($u-g$) for our whole sample (grey), and for the optical red sequence (pink). This essentially compares the slope of the SED at wavelengths above and below the u-band. In the bottom panel, we show the 'rectified' version, where we have removed the overall trend for the non-red sequence (i.e. star-forming) galaxies by plotting $y = $ (NUV$-u$) $- 1.7(u - g)$.

It is evident that 'blue cloud' galaxies actually follow a quite well-defined sequence in this colour-colour plot (cf. Salim et al. 2007), and that the extension of the sequence to redder ($u - g$) colours (which can reasonably be assumed to represent a lower, but non-zero, fraction of star formation) clearly runs into the area where optical red sequence, but 'NUV blue', objects lie.

We can therefore use these plots to improve our selection of truly passive objects. As a first cut we could remove from the red se-

quence those galaxies below $y = 0$ (the top of the main distribution for the 'blue sequence'). However, as a more cautious/stringent cut, we choose to also remove galaxies slightly above the bulk of star formers (perhaps shifted there through photometric errors, which are typically 0.2 magnitudes) via a cut at $y = 0.3$. Objects passing this cut are shown in red in the lower panel of Fig. 3. We will refer to the remaining subsample as the NUV red sequence galaxies. This subsample contains 147 of the original 265 optical red sequence galaxies.

To demonstrate the effect of the additional (NUV$-u$) cut, Fig. 2 above, also shows (in red) the histogram of the (NUV$-r$) colour for the NUV-selected red sequence. It is clear that making the additional cut in (NUV$-u$) vs. $(u - g)$ space has removed virtually all the objects with (NUV$-r$) below 5.0, which *post hoc* justifies the standard cut at the overall minimum in the (NUV$-r$) distribution when selecting genuinely passive galaxies (Salim 2014; Ali et al. 2019). Note particularly that (NUV$-r$) itself is *not* used in the selection at any point in this process (though of course (NUV$-u$) is). We can also note that the very few remaining galaxies with (NUV$-r$) < 5 in the NUV-selected red sequence are all at the faint end of our sample, with $M_r > -19.8$). This is likely due to the upturn component sitting on top of a lower metallicity old population (see Section 5, below).

Although we expect this cut to do a reasonably good job of excluding galaxies with residual star formation, it is obvious that *arbitrarily small* amounts of star formation will cause very small shifts from the colours of totally passive galaxies, so can *never* be ruled out from a single colour, or indeed a single colour-colour plot. If we add small but gradually increasing amounts of a star forming (flat spectrum) component to an assumed completely passive galaxy at the top right of the distribution in Fig. 3, it will initially move essentially vertically downwards (increase in NUV flux but no measurable effect on $(u - g)$, and then diagonally down and to the left, following the overall distribution that we, indeed, see for the pink points, consistent with them representing galaxies with small but measureable star formation, as we have assumed (see also Section 3.3 below).

As further confirmation that our chosen cut is appropriate, we have examined the (NUV$-u$) colours of the Coma Cluster early type galaxies with well-determined upturns from the multi-band ultraviolet SED fitting of Ali et al. (2018a). We find that the bluest colours among their upturn galaxies are (NUV$-u$) $\simeq 2.85$, corresponding to $y \simeq 0.3$, in excellent agreement with where we placed our cut in Fig. 3.

3.2 Mid-infrared Colours

We next check whether there may still remain galaxies with some residual effects of star formation. A totally independent measure of this is to use data from the *WISE* mid-infrared catalogues. *WISE* (W2$-$W3) colour is known to be an indicator of star formation through dust reprocessed emission (Jarrett et al. 2011; Cluver et al. 2014). In particular, Kettlety et al. (2018) demonstrated that a limit on (W2$-$W3) removed many galaxies otherwise thought to be passive systems. Fraser-Mckelvie et al. (2016) used similar constraints to search for passive spirals. The local nature of our sample ensures that *WISE* can detect all the galaxies in W3 even if they are passive (cf. the SINGS galaxy sample in Cluver et al. 2017).

Fig. 4 shows the (rectified) NUV-optical versus *WISE* colour-
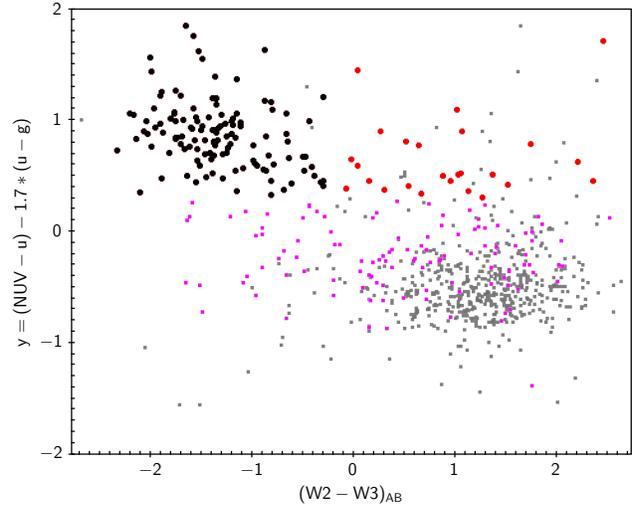
Figure 4. Rectified NUV-optical colour y versus *WISE* (W2-W3)$_{AB}$ colour for the various samples, plotted with the same colour codes as before. In addition the 122 objects from the NUV red sequence which also have *WISE* colours of non-star-forming galaxies are now plotted in black (the NUV+*WISE* red sequence sample). Although we do not impose a strict upper limit, errors in the *WISE* colours for our galaxies are less than 0.2 magnitudes in the large majority of cases. Errors in y are also around 0.2.

colour diagram for our various samples.[2] It is clear that many of the optical red sequence galaxies which had already been removed as potential star formers from their (NUV$-u$) colours (pink points) *also* have the (W2$-$W3) colours of star forming galaxies, as delineated by the grey points. In other words, the previously removed objects are indeed consistent with being low-level star formers.

In addition there is a tail of NUV red sequence galaxies (i.e. ones which were sufficiently red in (NUV$-u$) for retention) but which have the red (W2-W3) colours of star-forming galaxies. Removing these (the red points) leaves 122 red sequence objects which have both $y > 0.3$ *and* (W2-W3)$_{AB}$ < -0.3, the edge of the bulk of blue cloud objects (cf. Jarrett et al. 2011). We refer to these as NUV+*WISE* red sequence objects and these are shown in black in Fig. 4.

Referring back to the dark red (black bordered) histogram in Fig. 2, representing this final selection, it is evident that while a few of the bluer (NUV$-r$) objects have been removed by the *WISE* cut, the range for our 'double checked' passive sample remains the same as before, (NUV$-r$) from 5.2 to 6.5.[3]

In passing, it is interesting to note that if we return to the optical red sequence selection in $(g - r)$, the distribution (Fig. 5) is much narrower for the galaxies which have survived our cuts than it was originally (now only about $\pm 0.05^m$). It might be supposed, therefore, that a more refined choice from the original $(g-r)$ versus M_r colour magnitude diagram – selecting only from the redder side of the evident red sequence – might have achieved largely the same objective. However, the upper (redder) region of the optical red se-

---

[2] Note that in the GAMA database, *WISE* magnitudes have been converted to the AB system, rather than the Vega system used in the cited *WISE* based papers.

[3] As we have the spectral measurements available, we have also checked that our final sample galaxies have 4000 Å break measurements of the amplitude expected for passive galaxies, i.e. D4000 > 1.5 (Balogh et al. 1999).
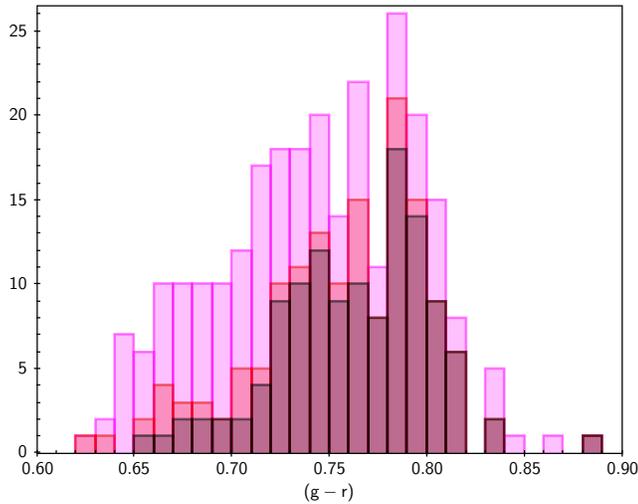
Figure 5. Histograms of the optical rest-frame $(g - r)$ colours for the various red sequence selections, colour coded as before. The final NUV+WISE sample has a significantly narrower range compared to the original sequence, but simply choosing galaxies redder than, say, 0.72 would still include potential weak star formers (pink and red histograms) in addition to the members of our 'best' sample (dark red histogram with black outlines). Photometric errors are around 0.03 magnitudes.

quence does still include significant numbers of galaxies which are removed by our other cuts, mixed in with our best passive systems.

As before, we can check the *WISE* mid-IR colours (Cutri et al. 2013) of the Coma Cluster upturn sample from Ali et al. (2018a). The reddest colours (so closest to the star-forming sequence) are at $(W2-W3)_{AB} \simeq -0.5$ (transforming to AB magnitudes using values in Jarrett et al. 2011), again close to our cut value of -0.3. (We might, therefore, have made a slightly tighter cut, though this makes virtually no difference in practice, with only nine galaxies having $(W2-W3)_{AB}$ between -0.5 and -0.3).

3.3 Specific Star Formation

The MAGPHYS assigned sSFRs averaged over the last 0.1 Gyr (Wright et al. 2016) for our final passive sample, while rather uncertain at such low levels[4], are virtually all below $10^{-11.4}$ yr^{-1}. Also the sSFRs do not correlate significantly with $(NUV-u)$, and at best weakly with $(W2-W3)$ (Pearson r coefficients -0.17 and 0.32, respectively), in contrast to what would be expected if significant SFR were evident (see Fig. 6). Indeed, the large majority of the values are consistent with the lowest allowed value in the modelling, 10^{-13}yr^{-1}, at the 3σ level. Furthermore, as the models do not contain an upturn component, if one is present, the fitting will presumably attempt to assign any extra ultraviolet flux to star formation instead. In that case, the true sSFRs are likely to be even lower than quoted.

Clearly, at these levels, the star formation rates cannot be expected to shift the $(NUV-r)$ colours by a magnitude or more from

[4] We can note, as validation of the MAGPHYS star formation rates, that they are consistent, even at low SFR, with those obtained from emission lines, where the latter are measurable (in the overall GAMA sample), see Wright et al. (2016) and Davies et al. (2016). For the star forming population, they also correlate as expected with the *WISE* colours.
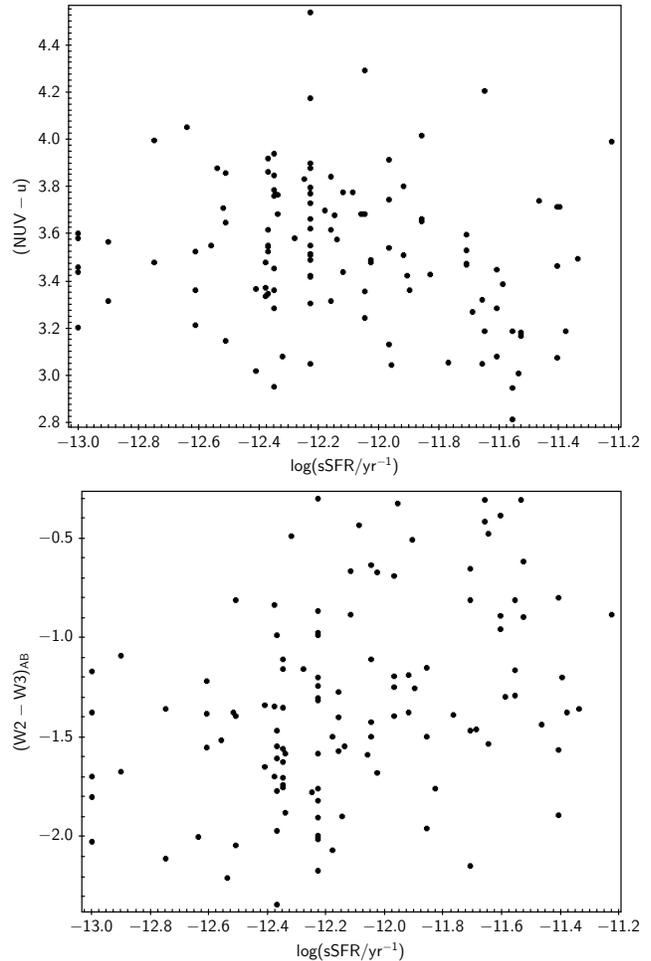
Figure 6. MAGPHYS derived specific star formation rates (averaged over the last 0.1 Gyr) plotted against rest-frame (NUV-u) colour (top panel) and $(W2-W3)_{AB}$ (bottom panel) for our final NUV+*WISE* red sequence sample.

those of the standard passive galaxy models (with no upturn) in order to cover the range of colours actually seen. To check this we can make a very simple calculation. We take the base $(NUV-r)$ colour of a totally passive galaxy with no upturn to be 6.75, from the models of Conroy, Gunn & White (2009) (see also Ali et al. 2018b), which effectively matches the upper limit for our data. Similarly for a star forming population, we take the bluest objects in our whole low z sample, which have $(NUV-r) \simeq 1.5$ and sSFR $\simeq 10^{-9}$yr^{-1}. Scaling this component down and adding it to the old population such that the overall sSFR $\simeq 10^{-12}$yr^{-1} (which is higher than that for the majority of our objects) we find a combined colour of 6.62, a change of only $\simeq 0.1$ magnitudes. Thus we cannot produce the bluer $(NUV-r)$ colours seen in our 'passive' sample by adding the observationally permissable amount of star formation. In other words, even if *very* low-level star formation exists (which can not be ruled out), its effects are much smaller than those from the upturn populations. The general lack of emission lines in our sample galaxies similarly implies that AGN activity cannot be a significant factor in the UV fluxes.

3.4 FUV

We can also consider the FUV output from our galaxies, though this significantly reduces the number available; in particular only 58 of our 122 NUV+*WISE* red sequence galaxies are detected with FUV errors less than 0.2 magnitudes (i.e. 5σ detections, as before).

In Fig. 7 we plot the distribution of (FUV-NUV) colours, where these are available, for galaxies in the various samples. It is evident that the star forming (blue cloud) galaxies (grey histogram) *and* most of the galaxies removed by our previous NUV and *WISE* cuts (pink and red histograms) are concentrated at (FUV-NUV) below 1.1 (cf. Brown et al. 2014). The final NUV+*WISE* red sequence galaxies (dark red histogram) span (FUV-NUV) from 0.7 to 2.1 (plus some even redder outliers). Being extra cautious we could remove from our best sample, the objects with (FUV-NUV) colours overlapping those of the star formers (which is actually the reverse of the Yi et al. (2011) criterion, as they keep only the bluest galaxies as upturns). However, it turns out that this does not change the (NUV $-r$) distribution, as the NUV+*WISE* red sequence objects above and below, say (FUV-NUV) = 1.1, have the same range in (NUV$-r$). This supports the suggestion of Smith et al. (2012) that there is a continuum of colours for the passive upturn galaxies, spanning (fairly) blue to red in (FUV-NUV). It also agrees with the range in (FUV-NUV) colour found by Boselli et al. (2005) for (non-dwarf) early-type galaxies in the Virgo Cluster and by Brown et al. (2014) for their local spectroscopic sample. We therefore keep the NUV+*WISE* red sequence sample as our best passive sample in what follows, without any extra constraint from the FUV.

We can note, however, that for our passive galaxies there is an essentially linear correlation between (FUV$-r$) – which undoubtedly measures the upturn population in passive galaxies with no star formation – and the (NUV$-r$) colour which we use in the rest of this paper, albeit with a significant scatter of around $\pm0.5^m$. Specifically, the bluest passive galaxies in (FUV$-r$), that is those with the strongest 'classical' FUV-determined upturns, are also the bluest in (NUV$-r$). Conversely, the reddest galaxies in both cases match the colours expected for models of standard metal-rich old populations (e.g. Conroy, Gunn & White 2009) with no upturn. This correlation between (FUV$-r$) and (NUV$-r$) is also seen for passive Coma Cluster galaxies with well characterised upturns in the sample of Ali et al. (2018a) and clearly supports our assertion that (NUV$-r$) is a good proxy for the upturn strength, even though also affected by the underlying old population (Burstein et al. 1988; Dorman, O'Connell & Rood 1995, 2003; Smith et al. 2012; Ali et al. 2019). Ali et al. (2018a) discussed in detail general two component SED models (i.e. with no star formation contribution), where the fits to the UV SED depend on both the metallicity and age of the old component and the strength (essentially the mass fraction of the relevant stellar sub-population) and temperature of the upturn component.

4 UPTURNS AND ENVIRONMENT

Having established that (NUV$-r$) colour is a suitable proxy for upturn strength and defined our best sample of non-star forming galaxies, it is evident that these galaxies, our best candidates for purely passive objects, with or without an upturn, span the same range of (NUV$-r$) colours as found for passive galaxies in local clusters by Ali et al. (2018a), who used more detailed ultraviolet SEDs which allowed them to rule out even very small amounts of star formation in their samples. Ali et al. (2019) further show that
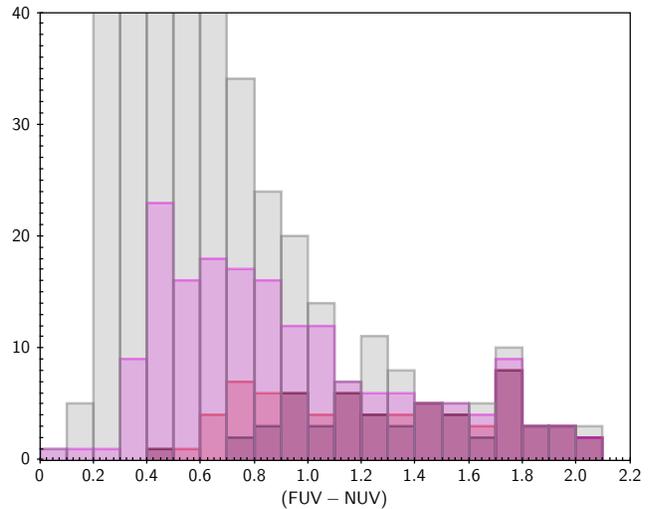
Figure 7. Distributions of (FUV-NUV) colour (where available) for the various samples, plotted with the same colours as before. (Note that the vertical scale has been truncated to allow the details of the three red sequence selections to be made clearer). Star-forming galaxies (grey histogram) can be seen to be concentrated at (FUV-NUV) < 1.1, as are the galaxies removed by our NUV and *WISE* colour cuts, while our NUV+*WISE* passive galaxies span the range $\sim$ 0.7 to 2.1. Colour errors here are up to 0.3 magnitudes.
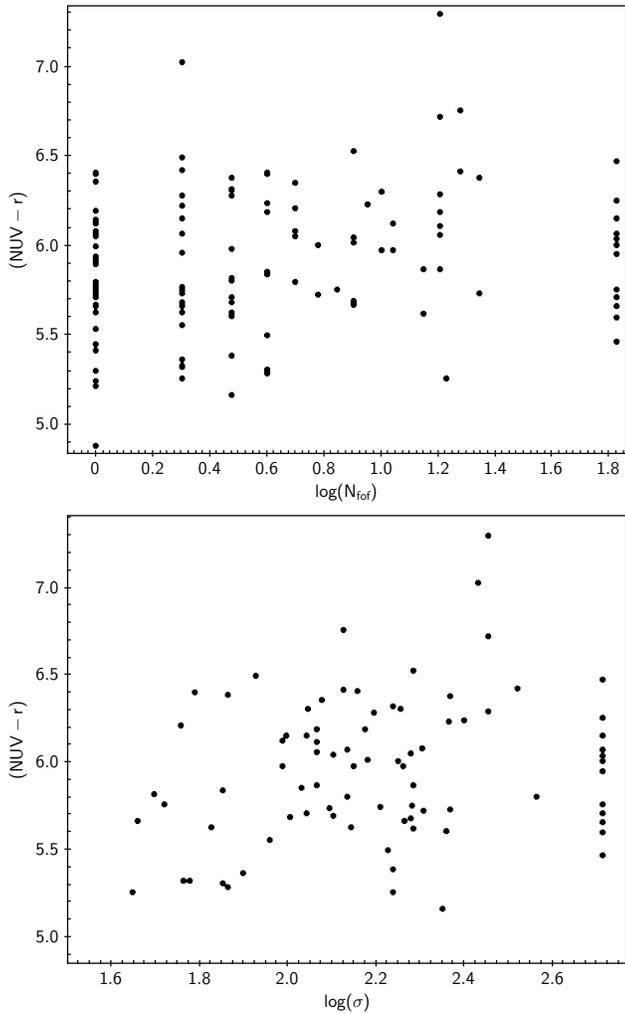
this colour range applies independently of the velocity dispersion or X-ray luminosity (essentially mass proxies) of the galaxies' host clusters (their Figure 4).

Fig. 8 demonstrates the same independence of environment (Pearson r coefficient 0.15) among our small group galaxies (only one group has more than 25 members). The upper panel shows the (NUV$-r$) colours as a function of group (friends-of-friends) multiplicity from Robotham et al. (2011). (Un-grouped galaxies are given a group multiplicity of 1, i.e. $\log(N_{fof})$ = 0). The lower panel matches the upper right panel of Figure 4 of Ali et al. (2019) and confirms that there is no dependence of the colour range on group velocity dispersion σ. This plot essentially continues the Ali et al. (2019) plot below their limit at $\sigma \sim 400$ kms^{-1} with exactly the same colour range. Using either an estimated virial mass or a measure of the total stellar light from the group galaxies results in the same lack of dependence (r < 0.15 in all cases).

This strongly reinforces the conclusion of Ali et al. (2019) that the UV upturn is a phenomenon internal to individual galaxies and is not affected by the larger scale environment in which the galaxy finds itself. Note that this differs from the case for slightly bluer objects, with (NUV$-r$) $\leq$ 5 and hence evidence for residual star formation, which *are* found to be environment dependent (e.g. Crossett et al. 2017, see also Donas, Milliard & Laget 1995).

To complete the comparison with the Ali et al. (2019) analysis of the (NUV$-r$) colours, Fig. 9 shows the colour range as a function of radial distance from the group centre, normalised by the group's effective radius (the radius containing half the galaxies), again from Robotham et al. (2011). Very small values are for galaxies near the geometric centre of their group: non-grouped galaxies are not plotted here, but we can already see their (matching) colour distribution from the previous plot (top panel, Fig. 8).

As in the upper right panel of Figure 5 of Ali et al. (2019) for cluster galaxies, we see no positional dependence of the (NUV$-r$) colours among the group galaxies (r = 0.15). Galaxies close to and relatively far from the group centre are equally likely to show the broad range of (NUV$-r$) colours which evidences the UV upturn.
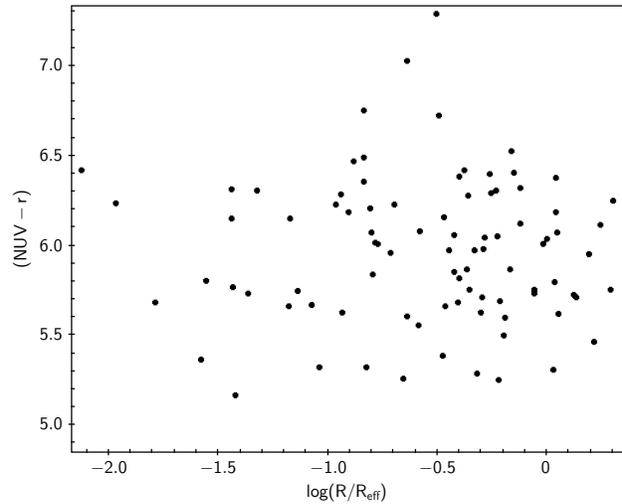
Figure 9. Distribution of rest-frame (NUV−*r*) colour for the passive NUV+*WISE* red sequence sample as a function of radial distance R, normalised by host group effective radius, $R_{\rm eff}$. This can be directly compared to the upper right panel of Figure 5 in Ali et al. (2019).

Figure 8. Distribution of rest-frame (NUV−*r*) for the final passive (NUV+*WISE* red sequence) sample versus the multiplicity of the group containing the galaxy (top panel), and versus group velocity dispersion σ (bottom panel). The bottom panel can be compared to the upper right panel of Figure 4 in Ali et al. (2019).
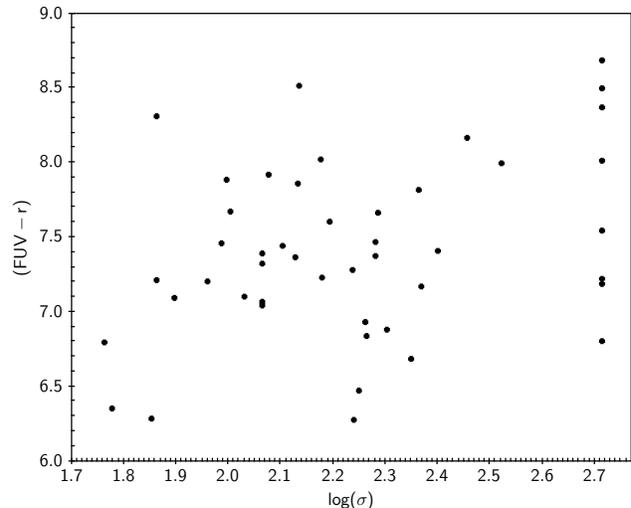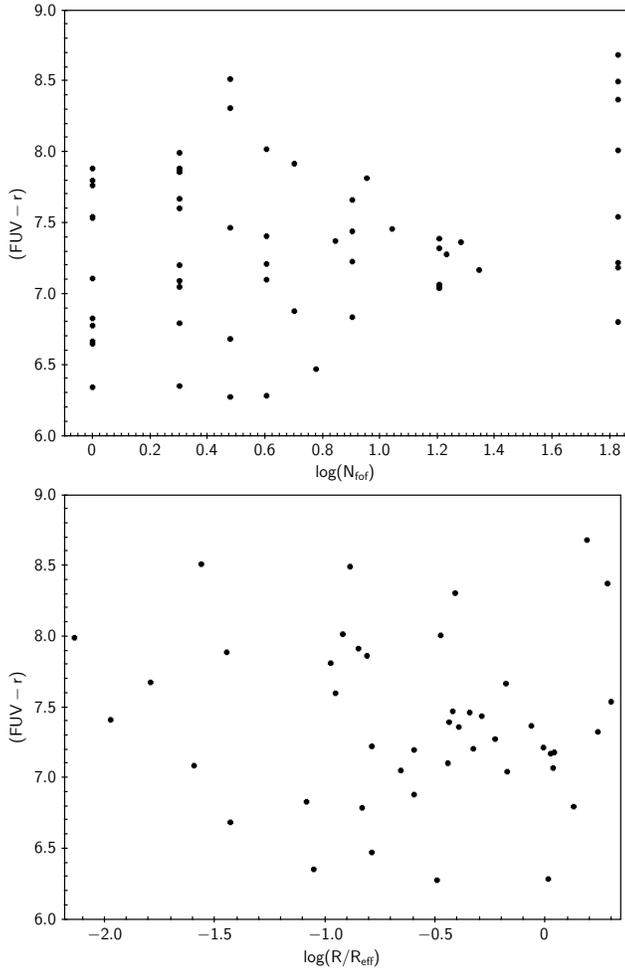

Figure 10. (FUV−*r*) colour (where available) versus the host galaxy group velocity dispersion for the final NUV+*WISE* red sequence sample. This can be directly compared to the upper left panel of Figure 4 in Ali et al. (2019).

We can repeat the exercise for the (FUV−*r*) colours of our sample galaxies, though the numbers with FUV detections are more limited. As an example, Fig. 10 shows the distribution of the FUV-optical colour versus the velocity dispersion of the galaxies' host groups. As with the NUV, we again see a wide spread of colours but no correlation (r = 0.04) of FUV-optical colour with environment (see also Atlee et al. 2009). FUV-optical colour against group multiplicity and radial position, Fig. 11, also show no effects (|r| < 0.1), again in agreement with the results of Ali et al. (2019) for larger clusters. Thus the FUV data in Fig. 10 and Fig. 11 independently supports the lack of environmental dependence of the upturn, regardless of any question of the contribution to the NUV fluxes, as used in the rest of the paper, from non-upturn components.

5   ADDITIONAL PROPERTIES OF UPTURN GALAXIES

As we have a wide range of other properties measured for our GAMA galaxies, it is of interest to make use of these to explore whether our apparently passive galaxies with relatively blue UV-to-optical colours are distinguished in any other way.

If we make use of the optical morphologies from Moffett et al. (2016) we find that all our NUV+*WISE* red sequence sample galaxies are classified either as E or S0/a, in essentially equal numbers. The range of (NUV−*r*) is the same in each case. Bureau et al. (2011) tentatively suggested that UV upturns were preferentially in slow rotators, but a substantial number of S0 galaxies also containing upturn populations may argue against this.

Using the Sérsic surface brightness profile fits from Kelvin et al. (2012) we find no correlation of the (NUV −*r*) colour of our final sample galaxies with their Sérsic indices in any optical band (e.g. Fig. 12), their central surface brightnesses or their axial ratios (Pearson |r| below 0.06 in each case). Thus, the presence of a strong upturn component does not seem to depend in any obvious way on the overall structure of the galaxy. This may possibly disfavour
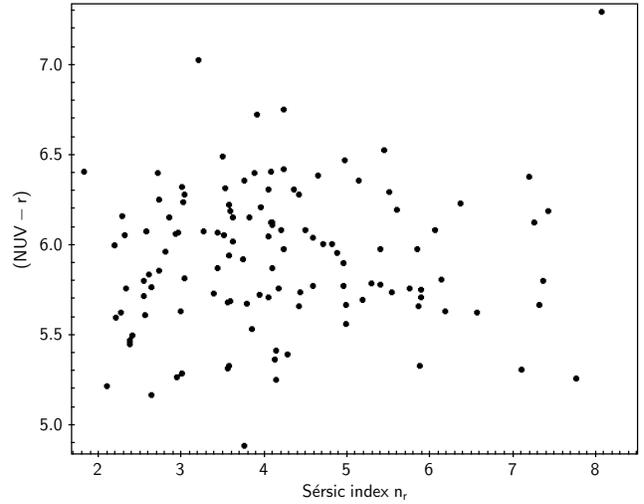
Figure 12. Distribution of rest-frame (NUV−r) colour for the NUV+*WISE* red sequence galaxies as a function of r−band Sérsic index.

Figure 11. (FUV−r) colour versus the host galaxy group multiplicity (top panel) and versus radial distance, normalised by group effective radius, (bottom panel) for the final NUV+*WISE* red sequence sample.

on which the star formation decayed (cf. Phillipps et al. 2019), or stellar metallicity.

The top panel in Fig. 13 shows that among our final sample (black points), there is no correlation between fitted age and the strength of the upturn (Pearson r = 0.09). However there is a clear trend for the optical red sequence galaxies which failed the (NUV −u) cut (pink points) to be modelled as having younger ages, as one might expect if they have (had) residual star formation. Note that these ages are determined by the total light, so do not necessarily reflect the age of the oldest stars, the UV upturn in particular being expected to result from HB stars at least 8 Gyr old (e.g. Kaviraj et al. 2007b; Ali et al. 2018c).[5]

For the star formation timescale, τ (middle panel), we again see that the bulk of the eliminated pink points (and most of the red circles, the galaxies which failed the *WISE* cut) tend to lie at larger values, consistent with longer lasting star formation, while the black points, our best (NUV+*WISE* red sequence) sample, generally ran down their star formation on timescales 1-2 Gyr. There is, here though, also a trend within the black points, with the tail of objects at (NUV−r) below 5.5 being among the galaxies with slightly longer τ. As these bluer objects are also typically less massive, as discussed below, this may be a consequence of general 'downsizing', i.e. smaller galaxies having more extended star forming lifetimes (Cowie et al. 1996). Unsurprisingly, given that the 'age' t is nearly constant for the passive galaxies, we see a corresponding distribution if we instead plot t/τ (Phillipps et al. 2019), again a measure of how evolved a galaxy is.

The stellar metallicities of our various red sequence sample galaxies are shown in the bottom panel of Fig. 13. Again, within the NUV+*WISE* red sequence objects (see the top panel of Fig. 14 for an expanded version), while there is a clear overall correlation, the *width* of the (NUV−r) colour distribution is similar at all metallicities, suggesting a similar range of upturn components superimposed on base models whose colours vary with metallicity. The Conroy, Gunn & White (2009) models imply that (in the absence

the alternative models for the upturn based on producing hot stars via envelope loss in close binaries (Han et al. 2007), if the binary fraction is dependent on, e.g., stellar density (Lucatello et al. 2015).

Visual inspection of our sample galaxies does not show any sign that major mergers play a part in the production of blue NUV colours. Also, regarding lower levels of disturbance, from potential past or more minor interactions, no relationship is found between the residuals from the smooth Sérsic models (as measured by the χ^2 goodness of fit) and the (NUV−r) colours and therefore upturn strength, implying that such interactions have played no part either. Given our previous results, this is, of course, as expected, since the interactions a galaxy will suffer are dependent on its overall environment.

Although we have many derived stellar population parameters from the Taylor et al. (2011) fits, it may not be entirely appropriate to consider correlations with these, as the models used in Taylor et al. (2011) do not include an upturn component. Nevertheless, to the extent that the models only use data longwards of 3000 Å, which should be reasonably unaffected by a separate UV upturn component, we can tentatively search for correlations between (NUV −r), measuring the strength of the upturn, and, e.g., the stellar population 'age' (time since the peak in star formation), the timescale τ

---

[5] A more precise measure of the oldest stellar population age might also be a useful discriminant between the He enriched models and alternative binary star evolution models, as the hot stars produced in the latter case need not be extremely old (Han et al. 2007, Li et al. 2013).
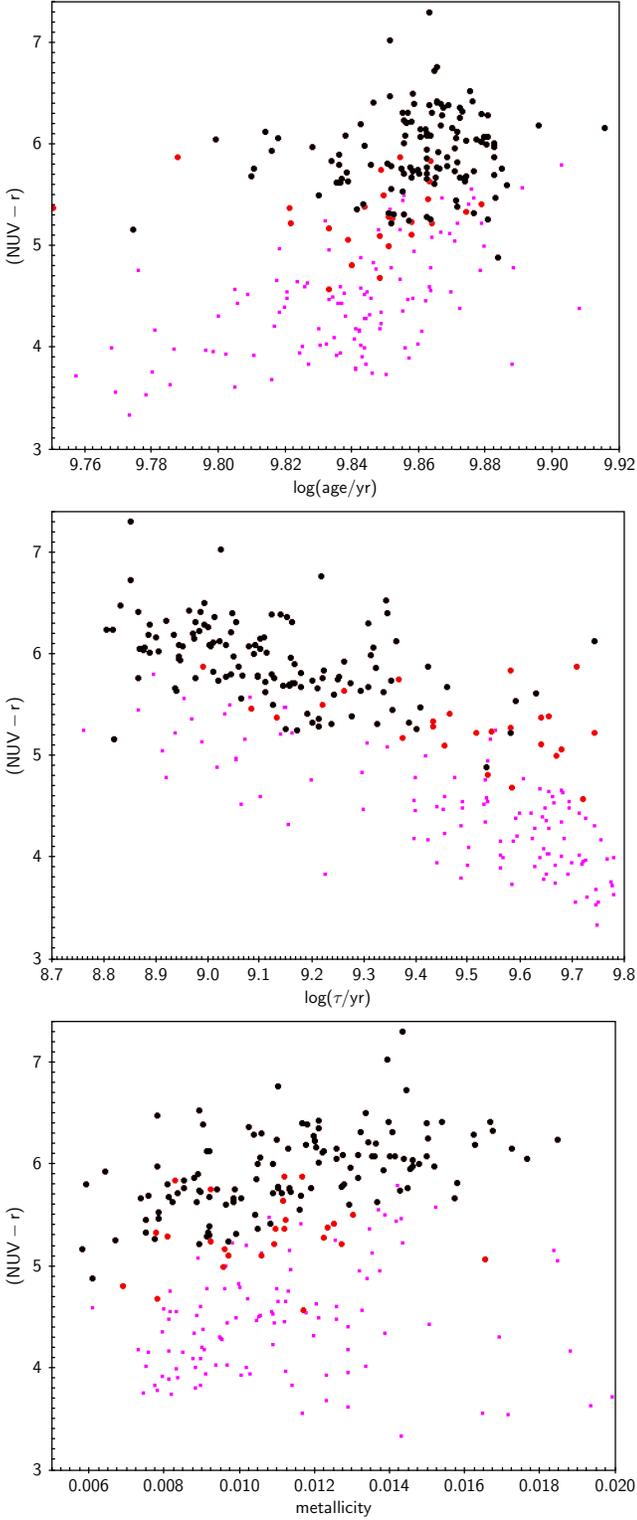
Figure 13. Distribution of rest-frame (NUV−r) colour for the three red sequence subsamples (coloured as previously) as a function of (top) stellar population age, (middle) star formation timescale τ, and (bottom) metallicity.
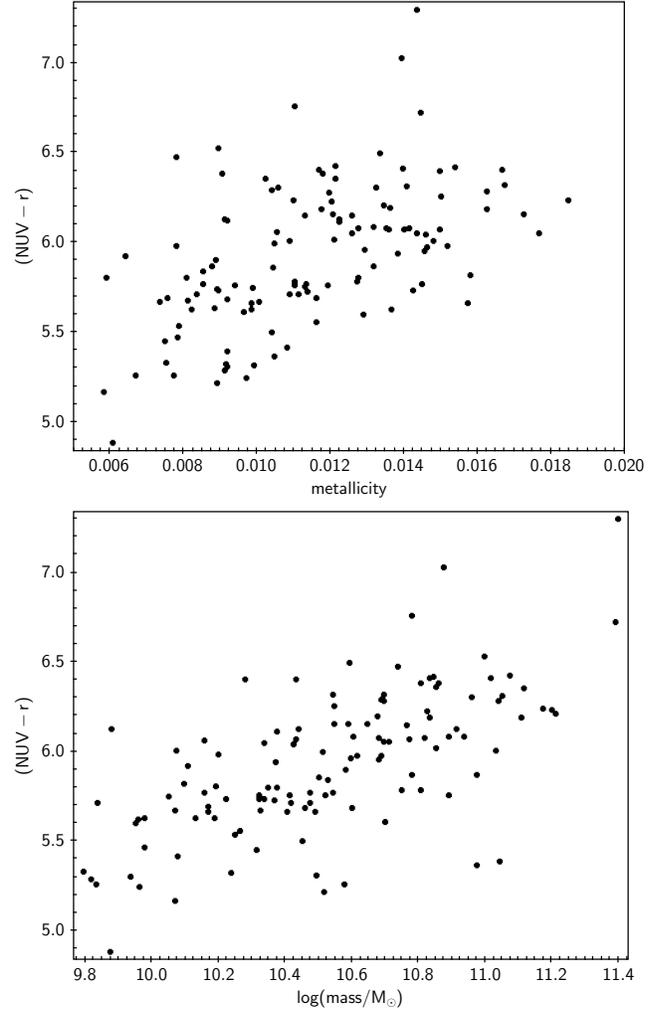
Figure 14. Distribution of rest-frame (NUV−r) colour as a function of stellar metallicity as in the bottom panel of Figure 11, but for the final NUV+*WISE* red sequence only (top panel), and as a function of stellar mass for the same sample (bottom panel).

of an upturn component) at old ages passive galaxies with half-solar abundances should be about 0.6 magnitudes bluer in (NUV−r) than solar metallicity objects, which is consistent with the slopes of both the red and blue envelopes of our data. This agrees with the implications of the work of Dorman, O'Connell & Rood (2003) who showed that the NUV SED will depend both on the strength of the upturn component and the metallicity of the old component (see their figure 1). The upper envelope in Fig. 14 then matches the colours of purely old populations of the various metallicities, without an upturn component. Note that the wide range of (NUV−r) colours at each metallicity appears to argue against the suggestion by Schombert (2016) that the upturn is *purely* a metallicity effect.

The few bluest (NUV−r) colours (below about 5.4) are all at the lower metallicity end and, unsurprisingly given the well known correlation of metallicity with mass (e.g. Faber 1973; Gallazzi et al. 2006), they are also at the low mass end of our sample (Fig. 14, bottom panel). From this plot, too, we see that there is a wide range of (NUV−r) at each mass (see Agius et al. 2013, for a similar plot in terms of luminosity).

Given all the caveats – especially that the population parameters are derived from a model which does not have an upturn

component – we therefore conclude that, within our best passive NUV+*WISE* red sequence sample, evidence for a correlation between the upturn stellar component and the underlying old stellar component is weak at best, *except* that lower mass (luminosity), lower metallicity passive galaxies extend to bluer UV-optical colours, and even this is likely due to the upturn component being superposed on a bluer background, rather than to a variation of the upturn component itself.

Finally, we make use of the MAGPHYS fits for the GAMA galaxies (da Cunha, Charlot & Elbaz 2008; Wright et al. 2016) for a number of ISM properties.[6] We find that among our final sample there is no correlation of blue upturn colour of our passive, early-type galaxies with any of dust mass, optical depth, temperature of the warm dust or temperature of the cold dust (Pearson $|r| < 0.15$ in each case). This is unsurprising given that the UV upturn is thought to be due to an old stellar population, so would not be expected to correlate with conditions in the present day ISM. We currently have no measurements of the neutral or molecular gas content of our sample galaxies.

6 DISCUSSION

The relevance of our results to the question of UV upturns in early-type galaxies is two-fold. First, we have shown how to empirically 'improve' a passive sample of galaxies, selected via the red sequence on a standard optical colour-magnitude diagram, by utilising additional constraints based on other broad band colours. Second, utilising our best passive galaxy sample derived in this way, we show that the range of (NUV$-r$) colours – which we interpret as reflecting the strength of an upturn components – is the same in all environments.

As our first additional constraint we used the (NUV$-u$) colour, essentially the slope of the spectrum shortward of 3000 Å. Specifically, from the distribution of galaxies in the (NUV$-u$) versus $(u-g)$ plane, we were able to extrapolate the locus of star forming galaxies and hence remove galaxies with residual star formation from the initial optical red sequence sample. By then using *WISE* (W2$-$W3) colours as an additional discriminant, we were able to further refine our non-star-forming sample. Within our final sample we find that galaxies with (NUV$-r$) < 5 have been eliminated, verifying *post-hoc* the frequent assumption that this value can be used as a convenient limit for upturn galaxies versus galaxies with residual star formation. This process also removes some galaxies with (NUV$-r$) > 5 which probably still have some star formation. Thus, as is well-known, unless more extensive data in the UV or IR is available, typically selected 'optically passive' samples, such as those we require in order to search for upturn galaxies, will not be entirely pure and even a selection based on (NUV$-r$) may still leave some galaxies with residual star formation. Our final sample contains only around half (122) of the original (265) galaxies selected to be on the optical red sequence in rest-frame $(g-r)$. This is consistent with the work of Mahajan et al. (2019) who find that around half of 'red' galaxies in their GAMA sample have spiral, rather than early-type, morphologies (see also Kaviraj et al. 2007a; Crossett et al. 2014).

Nevertheless, our 'best' passive sample demonstrates that early-type galaxies *do* still have a wide range of (NUV$-r$) colours even when the most stringent limits are placed on their residual star formation.

Additionally, it may be that we have removed galaxies which do have upturn components but which are confused by ongoing or recent star formation (i.e. they contain two UV emitting components). Note, though, that the (NUV$-r$) distribution of our final sample is quite steep on the blue side, which may indicate that few upturn galaxies with no star formation are lost. In addition, we suggest that further constraints using the FUV may not be appropriate.

Making use of our 'best' passive sample, derived in this way, our major result is then that (within the relatively low density environments sampled by the GAMA data) we find the *same* range of (NUV$-r$) upturn colours, from 5.2 to 6.5, irrespective of the environment, as measured by group multiplicity, velocity dispersion, or halo mass, or by position within the group. We find the equivalent result using a more limited sample of galaxies with sufficiently accurate (FUV$-r$) colours. This complements and extends to lower halo masses (including isolated galaxies), the results of Ali et al. (2019), who find no dependence of the range of upturn galaxy colours (and hence strength of upturn stellar component) with environment for galaxies in a wide range of nearby clusters. Thus the stellar population responsible for the upturn appears to be entirely defined by internal stellar evolutionary processes within galaxies, not, for instance, by additional populations produced via mergers or other environment/cluster dependent effects.

In addition, we find that the range of (NUV$-r$) colours is also independent (modulo the caveats noted above) of any (current) ISM properties, supporting the supposition that the upturn component is old. The overall galaxy (NUV$-r$) colours do depend on the stellar population metallicity, but the width of the distribution does not, implying the existence of UV upturn components with a similar range of strengths, superimposed on top of different underlying populations of varying (metallicity dependent) colour.

---

[6] We should not use the MAGPHYS stellar population properties in this context, as they are derived from the full wavelength range including the FUV and NUV, while the template models do not include an upturn population. We can use them for the dust properties as these are determined primarily by the far-IR data from Herschel-ATLAS (Eales et al. 2010).

REFERENCES

Agius N., Sansom A.E, Popescu C.C., et al., 2013, MNRAS, 431, 1929

Ali S. S., Bremer M. N., Phillipps S., De Propris R., 2018a, MNRAS, 476, 1010

Ali S. S., Bremer M. N., Phillipps S., De Propris R., 2018b, MNRAS, 478, 541

Ali S. S., Bremer M. N., Phillipps S., De Propris R., 2018c, MNRAS, 480, 2236

Ali S. S., Bremer M. N., Phillipps S., De Propris R., 2019, MNRAS, 487, 30211

Arnouts S., Le Floc'h E., Chevallard J., et al., 2013, A&A, 558, 67

Atlee D.W., Assef R.J., Kochanek C.S., 2009, ApJ, 694, 1539

Baldry, I. K., Glazebrook, K., Brinkmann, J., et al., 2004, ApJ, 600, 681

Baldry, I. K., Robotham, A. S. G., Hill, D. T., et al., 2010, MNRAS, 404, 86

Baldry, I. K., Driver, S. P., Loveday, J., et al., 2010, MNRAS, 421, 621

Baldry, I. K., Liske, J., Brown, M. J., et al., 2018, MNRAS, 474, 3875

Balogh M.L., Morris S.L., Yee H.K.C., Carlberg R.G., Ellingson E., 1999, ApJ, 527, 54

Bertola F., Capaccioli M., Oke J.B., 1982, ApJ, 254, 494

Boselli A., Cortese L., Deharveng J.M., et al., 2005, ApJ, 629, L29

Bremer M. N., Phillipps S., Kelvin L. S., et al., 2018, MNRAS, 476, 12

Brough, S., Croom, S., Sharp, R., et al., 2013, MNRAS, 435, 2903

Brown M.J.I., Moustakas J., Smith J.-D.T., et al., 2014, ApJS, 212, 18

Brown T. M., Bowers C. W., Kimble R. A., Ferguson H. C., 2000, ApJ, 529, L89

Brown T. M., Ferguson H. C., Smith E., Bowers C. W., Kimble R. A., Renzini A., Rich R. M., 2003, ApJ, 584, L69

Bruzual G., Charlot S., 2003, MNRAS, 344, 1000

Bureau M., Jeong H., Yi S.K., et al., 2011, MNRAS, 414, 1887

Burstein D., Bertola F., Buson L.M., Faber S.M., Lauer T.R., 1988, ApJ, 328, 440

Calzetti D., Armus L., Bohlin R. C., Kinney A. L., Koornneef J., Storchi-Bergmann T., 2000, ApJ, 533, 682

Carter, D., Pass, S., Kennedy, J., Karick, A.M., Smith, R.J., 2011, MNRAS, 414, 3410

Chabrier G., 2003, PASP, 115, 763

Chung, C., Yoon, S.-K., Lee, Y.-W., 2011, ApJ, 740, 45

Cluver, M. E., Jarrett, T. H., Hopkins, A. M., et al., 2014, ApJ, 782, 90

Cluver, M. E., Jarrett, T. H., Dale, D.A., Smith,J-D.T., August, T., Brown M.J.I., 2017, ApJ, 850, 68

Code A.D., Welch G.A., 1979, ApJ, 228, 95

Conroy, C., Gunn, J.E., White, M., 2009, ApJ, 699, 486

Cowie L.L., Songaila A., Hu E.M., Cohen J.G., 1996, AJ, 112, 839

Crossett J.P., Pimbblet K.A., Stott J.P., Jones D.H., 2014, MNRAS, 437, 2521

Crossett J.P., Pimbblet K.A., Jones D.H., Brown M.J.I., Stott J.P., 2017, MNRAS, 464, 480

Cutri R.M., Wright E.L., Conrow T., et al., 2013, Explanatory Supplement to the AllWISE Data Release Products

da Cunha E., Charlot S., Elbaz D., 2008, MNRAS, 388, 1595

Davies, L. J. M., Driver, S. P., Robotham, A. S. G., et al., 2016, MNRAS, 461, 458

De Propris, R., 2017, MNRAS, 465, 4035

De Propris, R., Bremer, M., Phillipps, S., 2018, A&A, 618, 180

Donas, J., Milliard, B., Laget, M., 1995, A&A, 303, 661

Donas, J., Deharveng, J.-M., Rich, R.M., et al., 2007, ApJS, 173, 597

Dorman B., O'Connell R.W., Rood H.J., 1995, ApJ, 442, 105

Dorman B., O'Connell R.W., Rood H.J., 2003, ApJ, 591, 878

Driver, S. P., Allen, P. D., Graham, A. W., et al., 2006, MNRAS, 368, 414

Driver, S. P., Popescu, C. C., Tuffs, R. J., et al., 2007, MNRAS, 379, 1022

Driver S.P., Hill D.T., Kelvin L.S., et al., 2011, MNRAS, 413, 971

Driver S.P., Wright A.H., Andrews S.K., et al., 2016, MNRAS, 455, 3911

Driver S.P., Andrews S.K., da Cunha E., et al., 2018, MNRAS, 475, 2891

Eales S., Dunne L., Clements D., et al., 2010, PASP, 122, 499

Eales S., Fullard A., Allen M., et al., 2015, MNRAS, 452, 3489

Edge, A., Sutherland, W., Kuijken, K., et al., 2013, The Messenger, 154, 32

Faber, S.M., 1973, ApJ, 179, 731

Fraser-McKelvie A., Brown M.J.I., Pimbblet K.A., Dolley T., Crossett J.P., Bonne N.J., 2016, MNRAS, 462, 11

Forrest B., Tran K.-V. H, Broussard A., et al., 2018, ApJ, 863, 131

Gallazzi, A., Charlot, S., Brinchmann, J., White, S.D.M., 2006, MNRAS, 370, 1106

Greggio L., Renzini A., 1990, ApJ, 364, 35

Han Z., Podsiadlowski P., Lynas-Gray A.E., 2007, MNRAS, 380, 1098

Hernández-Pérez, F., Bruzual G., 2014, MNRAS, 444, 2571

Hopkins, A. M., McClure-Griffiths, N.M., Gaensler, B.M., 2008, ApJ, 682, L13

Hopkins, A. M., Driver, S. P., Brough, S., et al., 2013, MNRAS, 430, 2047

Jarrett T.H., Cohen M,, Masci F., et al., 2011, ApJ, 735, 112

Kaviraj, S., Schawinski, K., Devriendt, J.E.G., et al., 2007a, ApJS, 173, 619

Kaviraj, S., Rey, S.-C., Rich, R.M., Yoon, S.-J., Yi, S.K. 2007b, MNRAS, 381, L74

Kaviraj, S., 2010, MNRAS, 408, 170

Kelvin, L. S., Driver, S. P., Robotham, A. S. G., et al., 2012, MNRAS, 421, 1007

Kelvin, L. S., Driver, S. P., Robotham, A. S. G., et al., 2014, MNRAS, 444, 1647

Kelvin, L. S., Bremer, M.N., Phillipps, S., et al., 2018, MNRAS, 477, 4116

Kettlety, T., Hesling J., Phillipps, S., et al., 2018, MNRAS, 473, 776

Lee, Y.-W., Joo, S.J., Han, S.-I., et al. 2005, ApJ, 621, 57

Leja, J., Tacchella, S., Conroy, C., 2019, ApJ, 880, 9

Lewis, I. J., Cannon, R. D., Taylor, K., et al., 2002, MNRAS, 333, 279

Li Z., Mao C., Chen L., Zhang Q., Li M., 2013, ApJ, 776, 37

Liske, J., Baldry, I. K., Driver, S. P., et al., 2015, MNRAS, 452, 208

Lucatello S, Sollima A, Gratton R., et al., 2015, A&A, 584, 52

Mahajan, S., Gupta, K. K., Rana, R., et al., 2019, MNRAS, in press

Moffett, A. J., Ingarfield, S. A., Driver, S. P., et al., 2016, MNRAS, 457, 1308

Morrissey P., Conrow, T., Barlow T.A., et al., 2007, ApJS, 173, 682

Norris, J.E., 2004, ApJ, 612, 25

O'Connell R.W., 1999, ARA&A, 37, 603

Phillipps, S., Bremer, M.N., Hopkins, A.M., et al., 2019, MNRAS, 485, 5559

Rawle T.D., Smith R.J., Lucey J.R., Hudson M.J., Wegner G.A., 2008, MNRAS, 385, 2097

Rich, R. M., Salim, S., Brinchman, J., et al., 2005, ApJ, 619, L107

Robotham, A., Driver, S. P., Norberg, P., et al., 2010, PASA, 27, 76

Robotham A., Norberg P., Driver S.P., et al., 2011, MNRAS, 416, 2640

Salim S., Rich R.M., Charlot S., et al., 2007, ApJS, 173, 267

Salim, S., 2014, Serbian Astronomical Journal, 189, 1

Salim, S., Rich M., 2010, ApJ, 714, 290

Saunders, W., Bridges, T., Gillingham, P., et al., 2004, Proc. SPIE, 5492, 389

Schawinski, K., Kaviraj, S., Khochfar, S., et al., 2007, ApJS, 173, 512

Schombert, J.M., 2016, AJ, 152, 214

Sharp, R., Saunders, W., Smith, G., et al., 2006, Proc. SPIE, 6269, 62690G

Smith R. J., Lucey, J.R., Carter D., 2012, MNRAS, 421, 2982

Sodré, L., Ribeiro da Silva, A., Santos, W.A., 2013, MNRAS, 434, 2503

Taylor, E. N., Hopkins, A. M., Baldry, I. K., et al., 2011, MNRAS, 418, 1587

Taylor, E. N., Hopkins, A. M., Baldry, I. K., et al., 2015, MNRAS, 446, 2144

Taylor M. B., 2005, ASPC, 347, 29

Tonry, J. L., Blakesee, J.P, Ajhar, E.A., Dressler, A., 2010, ApJ, 530, 625

Wright A. H., Robotham A.S.G., Bourne N., et al., 2016, MNRAS, 460, 765

Yi, S., Demarque, P., Oemler A., 1998, ApJ, 492, 480

Yi, S.K., Yoon, S.-J., Kaviraj, S., et al., 2005, ApJ, 619, 111

Yi, S.K., Sheen, J.-K., Jeong, H., Suh, H., Oh, K., 2011, ApJS, 195, 22